The shipping industry as a source of fine black carbon particles in the marine environment: a preliminary study for the case study of Saronikos Gulf.

Aikaterini-Anna Mazioti[1[0000-0003-0101-2145]] Vassilis Kolovoyiannis[1[0000-0001-5606-3754]], Vassilis Zervakis[1[0000-0001-7219-341X]], Evangelia Krasakopoulou[1[0000-0002-1948-3482]], Elina Tragou[1[0000-0003-0101-6410]], Risto Hänninen[2[0000-0001-8931-1726]], Mikhail Sofiev[2[0000-0001-9542-5746]], Elisa Majamaki[2[0000-0002-1470-555X]], Jukka-Peka Jalkanen[2[0000-0001-8454-4109]]

[1]Laboratory of Physical and Chemical Oceanography, Department of Marine Sciences, University of the Aegean, University Hill, 81100 Mytilene, Lesvos Island, Greece
[2]Atmospheric Composition Research, Finnish Meteorological Institute, Erik Palménin aukio 1, FI-00560 Helsinki, Finland
mazioti@aegean.gr, vkol@aegean.gr

Abstract. Black carbon is a product of incomplete combustion. BC particles remain suspended in the atmosphere and BC is considered among the major "climate active pollutants", influencing global climate change. In the current study, the atmospheric deposition of fine BC particles and their fate in the marine environment of Saronikos Gulf was investigated, combining atmospheric modelling outcomes with marine modelling tools. The contribution of the shipping industry to the atmospheric deposition mass balances of BC was examined, for the year 2018. For the area of Saronikos Gulf, it was found that the yearly production of fine BC by shipping activities was approximately two orders of magnitude lower compared to the total deposition mass flux of BC. The fate of this pollutant in the marine environment, due to transport processes, was examined by testing various configurations (i.e. particle settling velocities). The accumulation rate of fine particulate black carbon finally settling onto the top sediment layer was quantified for each configuration.

Keywords: Black Carbon Emissions, Marine Environmental Modelling, Delft3D, SILAM, Saronikos Gulf.

1 Introduction

Black carbon (BC) is a component of fine particulate matter, produced via incomplete combustion of fossil fuels, biofuels and biomass [1]. It is considered among the major "climate active pollutants", influencing global climate change [2, 3]. At the same time, BC is participating in the global carbon cycle, acting as a carbon sink due to its refractory characteristics and persistent nature [2, 4]. Regarding BC mass balances, the yearly global atmospheric emissions of BC particles are estimated to reach up to 29 Tg [5, 6]. Part of BC emissions are finally deposited to the surface of oceans, via wet and

dry deposition [6]. Jurado et al. [7] have estimated that the yearly deposition rates of BC to the surface of the oceans reach 2 Tg (dry deposition) and 10 Tg (wet deposition), on a global scale.

The size of emitted BC particles from various sources can vary from less than 10 nm [8] to some μm [9] or even one mm in case aggregates are formed [10]. The shipping industry contributes to BC fine particles emissions, with the greater part of BC particles emitted by ships falling within the range of some nm and up to 1000 nm [8, 11, 12]. Moldanová et al. [8] conducted onboard measurement campaigns and observed significantly greater abundance in the number of small sized particles (diameter up to 0.5 μm). Similarly, Xiao et al. [11] examined shipping emissions at berth and reported that the distribution of particles were ranging between 0.2 to 2.5 μm, presenting a skewed distribution with a peak appearing between 0.38 and 0.44 μm. Finaly, Eger et al. [12] examined inland ship emissions (Rhine River) and reported that particle size distribution in ship plumes was very low for particles with a diameter from 2.5 to 10 μm and that the majority of emitted particles were ultrafine particles with diameter smaller than 100 nm. The size of particles emitted by ships depends on the type of engines used onboard, the fuel type and the operational conditions [13, 14, 15]. Anderson et al. [13] reported that at low engine loads (lower than 35%), higher numbers of particles (ranging from 5.6 to 560 nm) were emitted, highlighting the importance of considering particle emissions in port areas. Regarding the influence of engine types, Rönkkö et al. [14] compared marine engines with maximum rated powers between 187 kW and 72 MW and reported that higher emissions were produced by two-stroke marine engines (manufactured in 1980s). Additionally, considering the influence of fuel type on emissions, low sulfur content in fuels as well as high quality fuels are associated with lower emissions of nanoparticles [13, 15]. With the use of open-loop scrubbers onboard, a part of the particulate matter produced by ship engines is expected to be discharged to the marine environment via the water stream [16], resulting to a proportion of BC being discharged directly into the water. Until the year 2019, only a small number of scrubbers were installed globally [17], therefore prior to the year 2019 the main pathway for BC to the marine environment due to shipping activity was through atmospheric emissions and the subsequent depositions.

Once in the marine environment, BC can be identified either in the dissolved or in the particulate phase. Particulate black carbon (PBC) acts as a sorbent for pollutants (trace metals, pesticides, PAHs and others) and nutrients, i) influencing their transport from the atmosphere to the sea and ii) altering their concentrations in the water column due to sorption/desorption processes [6]. Due to slow degradation, BC particles are expected to persist over time and are even found in deep-sea sediments [18, 19], while the dynamics and distribution of PBC in marine environments are not fully understood [20]. Additionally, PBC's reactivity with dissolved organic matter affects its availability in the water column as well as the growth and development of bacteria and phytoplankton [1], with the potential to influence the functioning of the ocean's biological carbon pump [6]. At present, there is considerable uncertainty about the behavior of PBC in the marine environment and the processes in which it is involved, as only limited studies have been carried out on PBC in seawater and sediments and for specific areas [6, 20, 21, 22]. Yang et al. [20] have investigated the dynamics of PBC

(distribution, settling speed, sinking flux) in the coastal Northeastern South China Sea, highlighting the slow-sinking characteristics of PBC in coastal waters and its decreasing offshore abundance. In a similar study, Fang et al. [21] examined the seasonal and spatial distribution of PBC in coastal China seas (Bohai Sea and Northern Yellow Sea), indicating higher concentrations of PBC during winter, attributing them to physical processes related to the East-Asian monsoon (e.g. resuspension of sediments). In the coastal area of Halong Bay (Vietnam), Mari et al. [6] studied the impact of wet deposition on PBC concentration in the water column. They have quantified increased concentration of PBC in the sea surface microlayer after rain events and they highlighted the potential of PBC to remove dissolved compounds (organic carbon, nitrogen, phosphorus and inorganic nitrogen and phosphorus) by sorption, altering thus their availability [6]. Another field study in the North Pacific Ocean (ALOHA station) pointed out the removal of dissolved BC from the water column via processes such as the vertical export on sinking particles [22], influencing in the long term the concentrations of BC found in the sediments. The study of the fate of PBC in the marine environment requires a synthetic approach combining atmospheric measurements and simulations/predictions with *in situ* measurements in the water column and sediments and marine modelling tools.

In the current study, the deposition and subsequent fate of BC in Saronikos Gulf (Eastern Mediterranean) was investigated. Located adjacent to the wider Metropolitan Area of Athens (central Greece), Saronikos Gulf receives high environmental pressure and at the same time is of high ecological value [23]. Apart from direct discharges and point pollution sources located on the coastal area [24], the Gulf receives pollution loads occurring from industrial and domestic activities taking place in the Attica region via atmospheric deposition [25]. While the water quality of Saronikos Gulf is being monitored on a frequent basis [26], only few modelling studies exist [24 and references therein]. To the best of our knowledge, so far there are no modelling studies focusing on the deposition and subsequent fate of BC in this marine area.

The implementation of this study as well as the results are presented within this article, structured with the following sections. The methodology section, where the study area is described; the atmospheric emission estimations and simulations set-up are described; the marine modelling tools used are presented. The results and discussion section, where the estimations of BC atmospheric deposition onto the surface marine layer is presented and discussed; the transport of BC within the marine environment (water column and sediments) is presented and discussed. The conclusion section where major conclusions are summarized.

2 Materials and Methods

2.1 Study area

Saronikos Gulf is located in the Aegean Sea (E. Mediterranean), covering an area of approximately 2800 km^2 (Figure 1). The Gulf can be divided in four sub-basins, i) Elefsis Bay, a shallow gulf (max 30 m depth) with intense industrial activities on the coast, ii) Inner Saronikos Gulf, receiving pressures from the metropolitan area of

Athens, the outfall of a wastewater treatment plant serving 5.6 million persons equivalent and the marine traffic occurring around Piraeus area, iii) Outer Saronikos, including the area from Aegina Island up to the "open boundaries" connecting Saronikos Gulf with the Aegean Sea, and iv) Western Saronikos, the marine area on the west of Salamina and the north of Methana and Aegina Island.

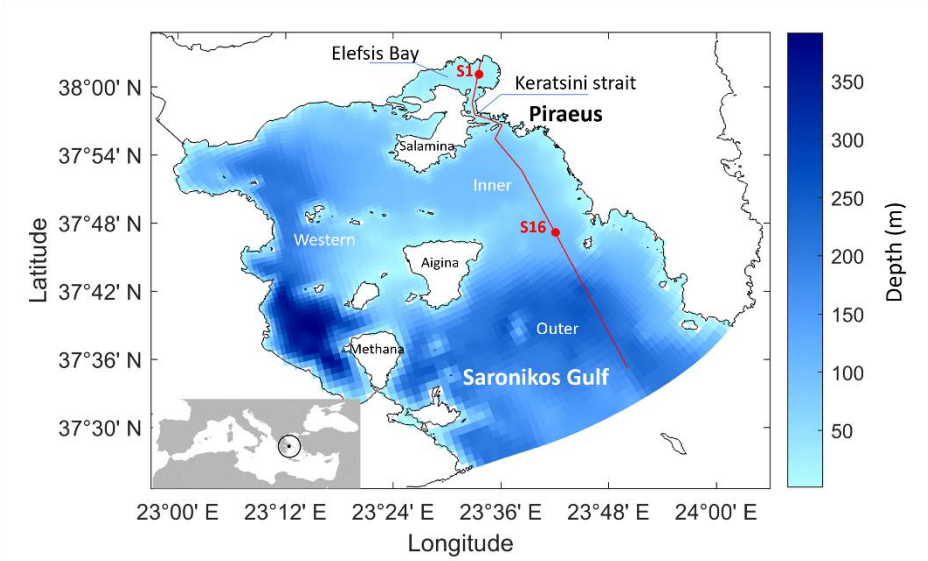

Fig. 1. Location and bathymetry of the study area, Saronikos Gulf, interpolated onto the curvilinear grid used in simulations. Vertical distributions of Black Carbon concentration are plotted along the cross section designated by the red line, and observation points S1 and S16 (red dots-labels) are used to further examine simulation results. This figure is a modification of Figure 1 from Mazioti et al. [24].

2.2 Atmospheric Emissions simulations

The atmospheric emissions of BC fine particles (nominal diameter 0.5 μm, defining a bin with limits 0.1 and 1.0 μm and considering a flat size distribution between these limits) from both background pollution and shipping activities were estimated for the year 2018 with the SILAM model, within the implementation of the Horizon 2020 EMERGE project [27]. The atmospheric concentrations and surface deposition fluxes of BC have been quantified for the extended region around Attica, Greece (Figure 1), as discussed below.

2.2.1 Model description

The atmospheric modelling component employed in this study is the System for Integrated modeLling of Atmospheric coMposition SILAM v.5.8 [28]. SILAM is a Eulerian chemical transport model that employes the Carbon Bond Model, version 05 (CBM05) to describe the chemistry of the troposphere [29]. It includes a set of supplementary tools including a meteorological pre-processor, input-output converters,

reprojection and interpolation routines, etc. A system description can be found at http://silam.fmi.fi.

2.2.2 Simulations setup

Simulations over the study area (shown in Figure 2) were carried out at high resolution of 0.05 × 0.05 degrees at the European scale at 10 different levels with boundaries taken from the CAMS IFS-model. All the runs had a one-hour temporal output resolution. SILAM runs were forced by meteorological fields from the IFS (Integrated Forecast system) model by ECMWF (The European Centre for Medium-Range Weather Forecasts) [30]. Hourly data from single forecast product at 9 km resolution was used for meteorological parameters like wind, temperature, humidity, cloud-fraction, and precipitation, plus different surface parameters. Shortest possible forecast length was used, making use of the forecasts provided at midnight and at noon.

Within the framework of the EMERGE Horizon 2020 project, two runs for the year 2018 were performed to examine the impact of shipping, with the first run incorporating both land emissions (anthropogenic and natural emissions) and shipping emissions from the STEAM model [31]. As shipping emissions are not included in the second run, the shipping contribution can be calculated by comparing the results of the two runs. To quantify the annual BC contribution of shipping, i.e. calculate the total mass deposition of BC on the sea surface of the study area originating only from shipping in 2018, the difference between the depositional mass fluxes of the two runs was calculated (SILAM depositional fluxes with shipping minus SILAM depositional fluxes without shipping) with purpose-built numerical tools. SILAM employed the Copernicus Atmospheric Monitoring Services (CAMS) regional emissions inventory (version 4.2) to estimate anthropogenic and natural emissions. Hourly STEAM emissions complemented CAMS emissions for the maritime industry. This process produced the necessary simulated concentration fields of fine BC in the air for 2018, with and without shipping emissions, that were used in each case to calculate deposition fluxes to the sea surface. Both the dry and wet deposition rates are included in the deposition statistics.

Currently SILAM considers BC as passive aerosol that is advected and deposited by dry- and wet depositions based on method by Kouznetsov and Sofiev [32]. Additional maximum scavenging rate is applied in order to avoid over-scavenging due to rains. Hourly shipping emissions from the STEAM model (including BC emissions) contain two altitude heights (from 0 to 36 m and from 36 m to 1000 m) where the emissions are inputted and then advected. This separation was done to incorporate emissions from smaller vessels (small passenger ships, leisure boats) in a lower atmospheric layer and emissions from larger vessels (cargo, large passenger ships) in a higher atmospheric layer, using layer boundary thresholds (e.g. 36 m) from past simulation efforts employing other widely used models (e.g. CMAQ, Community Multiscale Air Quality). All the standard anthropogenic emissions have sector-wise predefined monthly, weekly, and diurnal profiles, together with emissions altitude profiles that are also sector dependent.

Finally, three-dimensional files were created (one for each numerical experiment), containing the time-dependent depositional flux values (g m^{-2} d^{-1}) for each grid cell in

the case study area (Figure 1) with a 6 hours timestep, to force water quality simulations.

2.3 Marine Modelling Tools

The three-dimensional modelling suite Delft3D was implemented. The Delft3D-FLOW module was used as described in a previous study [24, 33], to reproduce the hydrodynamic conditions of the modelling area for the year 2018. The numerical model simulates the three-dimensional unsteady flow and transport phenomena resulting from meteorological and tidal forcing, including the effect of density differences due to a non-uniform temperature and salinity distribution (density-driven flow). It solves a system of non-linear equations consisting of the horizontal equations of motion, the continuity equation, and the transport equations for conservative constituents, derived from the three-dimensional Navier-Stokes equations for incompressible, free surface flow [34]. An 83×101 curvilinear grid was used, with a varying horizontal resolution from 1400 m to less than 300 m, able to resolve water mass exchanges between Elefis Bay and broader Saronikos. In the vertical direction, 20 σ-layers resolve the water column. Data from the ECMWF ERA5 database were used as atmospheric forcing fields, while the lateral oceanic boundary conditions were determined from an inhouse implementation of the Regional Ocean Modelling System (ROMS) covering the Central - North Aegean, with model setup as described in [35]. The Delft3D-WAQ module was coupled offline to the FLOW module, and BC fine particles were introduced at the sea surface in the form of depositional fluxes. As a first approach, only the physical mechanisms (advection and settling) were considered for the investigation of BC's fate in the marine environment. Based on these processes, the overall transport rate of PBC mass (g s^{-1}) was computed across each grid cell, taking into consideration the concentration of PBC, the cell surface area, water velocity and the turbulent diffusion coefficient [36]. The sedimentation of PBC was quantified according to Equation 1 [36, 37] and with the adoption of different settling velocities (Table 1).

$$D = w_s \cdot c \cdot \left(1 - \frac{\tau_b}{\tau_c}\right) \qquad \text{[Equation 1]}$$

where:

D deposition flux of black carbon [g m^{-2} d^{-1}]
w_s settling velocity of particulate black carbon [m d^{-1}]
c concentration of black carbon [g m^{-3}]
τ_b bottom shear stress [Pa]
τ_d critical shear stress for deposition [Pa]

Table 1. Settling velocities values used for the respective simulation scenarios [38, 39, 40]

	RUN1	RUN2	RUN3	RUN4
w_s [m d^{-1}]	0	0.1	1	function

To investigate the flocculation effect on the settling velocity, Equation 2 was used [41].

$$w_s = ftemp \cdot fsal \cdot fcon \cdot w0_s \quad \text{[Equation 2]}$$

where:

$$ftemp = kt^{(T-20)} \quad \text{[Equation 2a]}$$

$$fsal = \left(\frac{a_i + 1}{2}\right) - \left(\frac{a_i - 1}{2}\right) \times cos\left(\frac{\pi \times S}{Smax}\right) \quad \text{[Equation 2b]}$$

$$fcon = \left(\frac{C_S}{C_{SC}}\right)^{n_i} \quad \text{[Equation 2c]}$$

where:

a	coefficient for the enhancement of flocculation [-]
C_S	concentration of total suspended solids [gDM m^{-3}]
C_{SC}	critical concentration of total suspended solids above which flocculation occurs [gDM m^{-3}]
$fcon$	function for the concentration dependency of flocculation [-]
$fsal$	function for the salinity function dependency of flocculation range [-]
$ftemp$	function for the salinity function dependency of flocculation range [-]
kt	temperature coefficient for settling (water density correction) [-]
n_i	constant for concentration effect on flocculation [-]
S	salinity [psu, g kg^{-1}]
$Smax$	salinity at which the salinity function is at its maximum [g kg^{-1}]
T	water temperature [°C]
i	index for substance (*i*)

The user-supplied settling velocity ($w0_s$) was set to 1 m d^{-1} and coefficients related to the flocculation effect in relation to salinity, total suspended solid (TSS) concentration and water temperature (density effect) were set to be relevant with the modelling area and according to WAQ manual recommendations [41]. For this simulation (RUN4), a time series file representing the variable TSS concentrations was used, as developed in a previous study [24].

3 Results and Discussion

3.1 Atmospheric deposition of BC

The atmospheric deposition fluxes expressed as yearly rates (g m^{-2} y^{-1}) are presented in Figure 2. BC fine particles (0.5 μm) annual deposition from all sources, including coastal activities and shipping activities, reached the order of tens of mg per m^2 (Figure 2a). On the other hand, the contribution of shipping emissions to this mass balance was low (approximately 2 orders of magnitude lower), reaching the maximum rate of 0.5 mg per m^2 y^{-1} in some areas, e.g. in the northern parts of the domain. It is worth

mentioning that in the current study, only fine particles of BC (0.5 μm) were investigated, while larger particles, emitted from various sources other than shipping were not considered. As a result, BC mass balances computed in the current study are expected to be lower compared to other studies, where depositional fluxes are calculated through field measurements that include all particle fractions of BC [20].

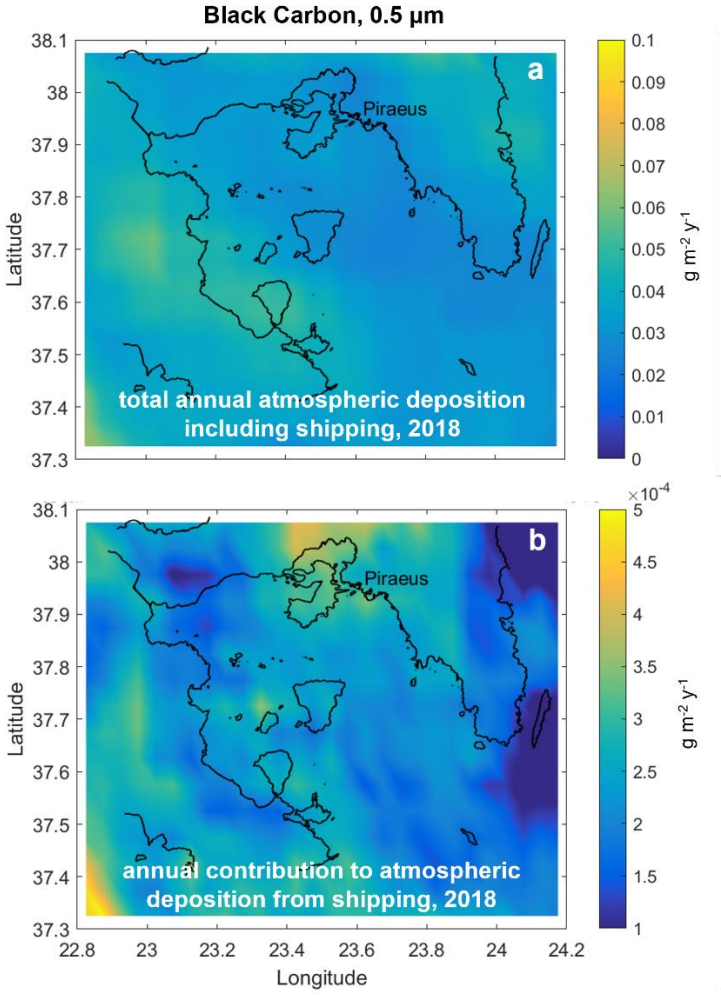

Fig. 2. Annual mass deposition (g m^{-2} y^{-1}) of Black Carbon fine particles as quantified by the SILAM atmospheric chemistry transformation model occurring a) from all sources (background and shipping), and b) from shipping activities. Note the different scales in the subfigures

3.2 Transport of BC in the marine environment

The atmospheric BC deposition fluxes to the marine surface layer were the sole source of BC pollution for this modelling set-up. To investigate the sensitivity of the model results to the settling velocity parameterization, different settling velocities of the particles were tested (Table 1). Initially, the assumption that the particle is not settling and is only subject to passive transport was tested (RUN1). Another approach examined the fate of PBC subject to settling processes with a settling velocity of 1 m d^{-1} (RUN3). Results from these two simulations can be seen in Figure 3, where the concentration of PBC in the water column in a section across the modelled area is illustrated (the section is indicated in Figure 1). It is evident that the lack of settling leads to higher concentration of PBC in the water column (Figure 3a) as the particles remain suspended and never settle, particularly in the enclosed Elefsis Bay where higher water renewal times prevail due to lower horizontal dispersion dynamics. On the contrary, when fast settling is considered, concentrations of PBC in the water column are lower (Figure 3b), as particles slowly sink and finally settle to the top sediment layer. The influence of open boundaries can also be observed in Figure 3, as in the current study it was assumed that the concentration of BC at the open boundaries is equal to zero, an assumption that is not realistic but is inevitable, due to lack of PBC field data measurements.

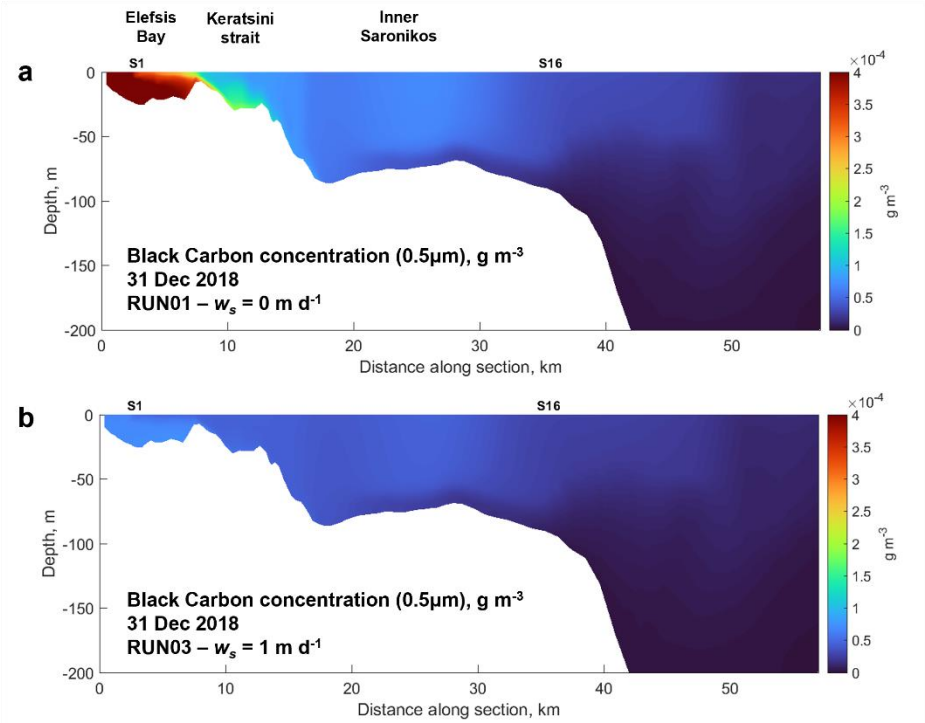

Fig. 3. Concentration of fine Black Carbon in the water column (g m^{-3}) along the cross section designated with red in Figure 1 on the last day of 2018 (annual simulation), a) assuming zero settling (w_s = 0 m d^{-1}, RUN1) and b) settling velocity of the particle w_s= 1 m d^{-1} (RUN3).

The concentration of PBC in the water column of Elefsis Bay (Figure 3) varied from 0.1 μg L^{-1} to 0.4 μg L^{-1}. Unfortunately, there are no available PBC concentrations for the study area based on water column sampling. Although it is quite dicey to compare with *in situ* data from other regions of the world ocean, where the whole size continuum of the bulk PBC has been determined (and not only the 0.5 μm size fraction), surprisingly the modelled PBC concentrations in Elefsis Bay fall within the same order of magnitude as those reported for the western Arctic and Subarctic Oceans, areas less affected by anthropogenic activities where PBC larger than 1 μm was determined [42].

To investigate spatial differences as well as differences due to parameterization, simulated time-series from two observation points were compared (S1 and S16). In both cases, the particle accumulation in the sediment layer (mass in g as a function of time) and the annual variability of deposition fluxes (g m^{-2} d^{-1}) were calculated for all the tested settling velocities. In the first case, an observation point in the shallow, semi-enclosed and environmentally vulnerable Elefsis Bay (S1, max depth 23 m) was investigated. As a second observation point, S16 was chosen, a location between Inner and Outer Saronikos Gulf (max depth 85 m), receiving lower pressure than S1 and influenced by the open boundaries water circulation, where PBC concentration was assumed to be equal to zero (Figure 4). As expected, in all cases, the assumption that the particles are not settling (RUN1) results in zero mass deposition in the sediment layer. Similarly,

when the settling velocity was calculated according to Equation 2 (computed w_s varying from 0.5 $\times 10^{-3}$ m d^{-1} to 16 $\times 10^{-3}$ m d^{-1}) and the above-mentioned parameterization (section 2.3), the deposition mass and fluxes are very low. In Figure 4a, referring to Elefsis Bay where bottom depth is 23 m, we can observe that for both simulations with close to zero settling velocities (w_s=0 and w_s=*function*) the particle is not accumulated in sediments and remains suspended in the water column. On the other hand, settling velocities of 0.1 m d^{-1} and 1 m d^{-1} led to annual accumulation of up to 5 and 25 mg m^{-2} of BC at station S1 respectively. Lower annual mass load deposition of PBC to the sediment was calculated at S16, with the higher being 5 mg m^{-2}. In Figure 4b, we can observe a similar trend when low settling velocities were implemented (w_s=0, w_s=0.1 and w_s=*function*) resulting to very low PBC mass deposition to the sediment layer. This can be explained taking into account the greater bottom depth of this part of Saronikos Gulf (S16, depth greater than 85 m), the different hydrodynamic circulation and the hydrodynamic exchanges with the open-sea (open boundaries) leading to PBC loss from the modelling area.

Regarding depositional fluxes over different time periods, seasonal variability can be observed (Figure 4 b, d). As an example, at S1 for w_s = 1 m d^{-1} (RUN3, Figure 4b), the flux varies from 0.02 mg m^{-2} d^{-1} (7.3 mg m^{-2} y^{-1}) during summer months to 0.16 mg m^{-2} d^{-1} (58.4 mg m^{-2} y^{-1}) during winter months. This variation may be related to the seasonality of atmospheric deposition fluxes of BC. An alternative cause of the observed variability could be summer stratification, which isolates to some extent the near-bed layers from the sea-surface conditions and the exchanges with the atmosphere.

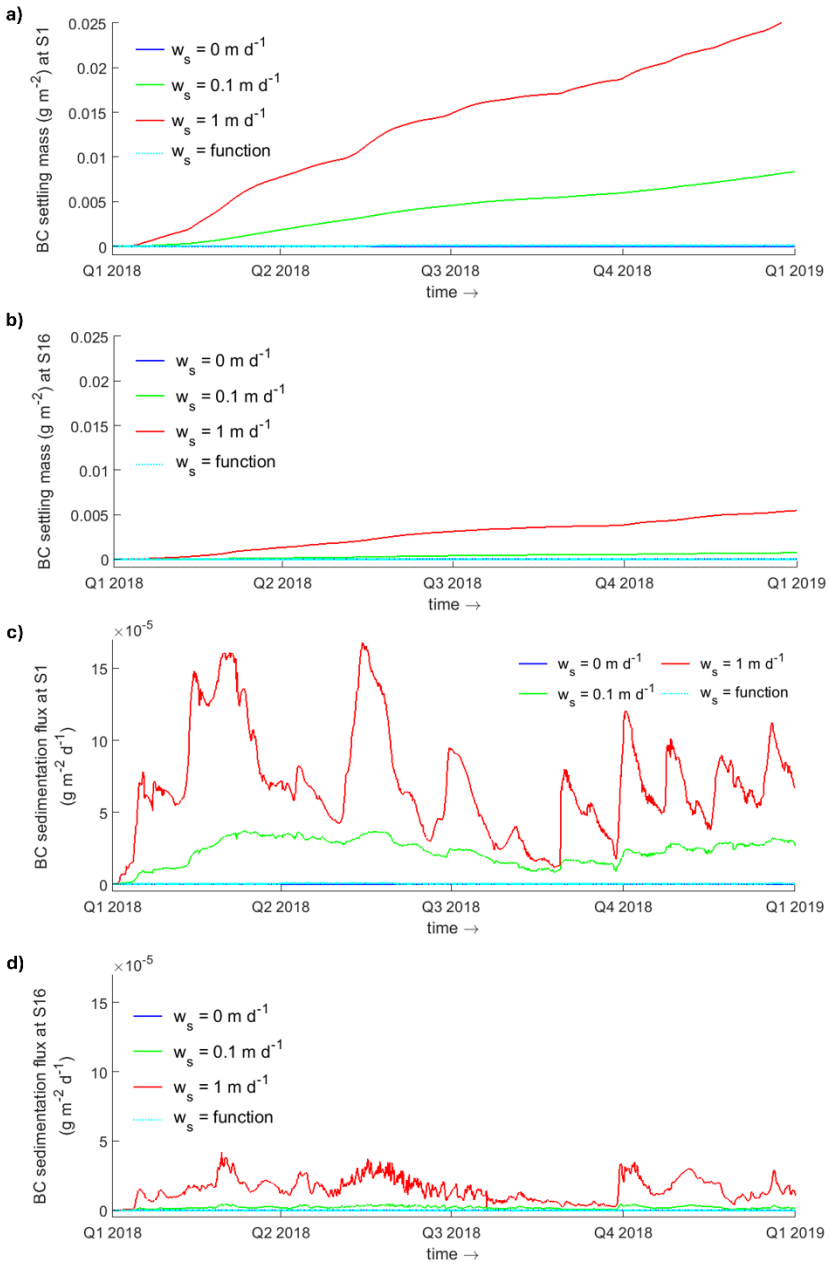

Fig. 4. Fine Black Carbon (0.5µm) settling mass (g) a) at S1 and b) at S16, and sedimentation flux (g m^{-2} d^{-1}) c) at S1 and d) at S16, to the top sediment layer over simulation time and different settling velocities. Quarters correspond to months as follows: Q_1 is JFM, Q_2 is AMJ, Q_3 is JAS and Q_4 is OND.

The spatial differences of sediment deposition of PBC are clearly shown on the relative maps that were created (Figure 5). The higher fluxes are recorded in Elefsis Bay, where a small volume of water (Elefsis Bay), receives relatively high BC loads through atmospheric deposition. Conversely, in other parts of Saronikos Gulf, lower fluxes are observed, for example Outer Saronikos, where the circulation of water from the open boundaries (with zero PBC concentration) decreases the PBC concentration, thus decreasing PBC availability for deposition to the sediment layer. Semi-enclosed bays, like Elefsis Bay, are considered to be effective traps for PBC (and associated contaminants as well) that is deposited in the local sediments [2].

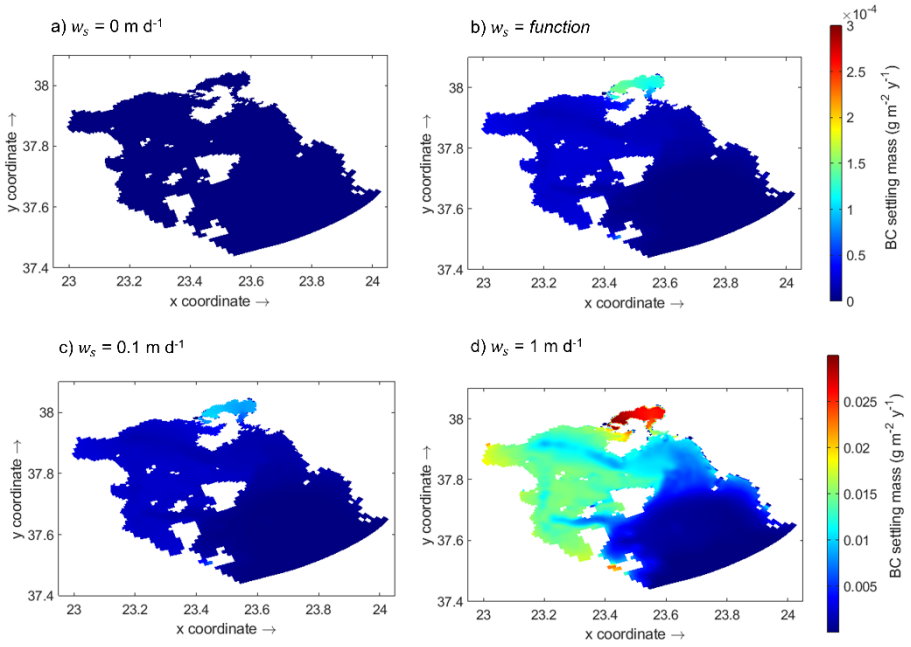

Fig. 5. Spatial distribution of PBC mass settled on the top sediment layer (g m^{-2} y^{-1}) after one year of simulation for each settling velocity a) w_s = 0 m d^{-1} (RUN1), b) w_s = *function* (RUN4), c) w_s = 0.1 m d^{-1} (RUN2), and d) w_s = 1 m d^{-1} (RUN3). Note the different scales in the subfigures in the upper (a, b) and lower (c, d) panel.

A factor that controls the PBC mass settled on the top sediment layer is the settling velocity of PBC. The only published attempt to quantify the PBC settling velocity in seawater revealed that settling velocity ranged from meters to tens of meters per day, illustrating the slow-sinking characteristics of PBC [20]. Using the literature available PBC datasets and a settling speed of 5.6 m d^{-1}, Yang and his coworkers [20] estimated the sinking flux of PBC at several shelves around the globe covering regions with low human activity (like the Arctic shelves) and hotspots of BC emissions (like the coasts of China). The estimated PBC sinking flux varied from 0.88 to 66.4 g m^{-2} y^{-1}, spanning 1-2 orders of magnitude. In the present study, the settling velocities employed were much lower than the speed used by [20], thus leading to lower deposition fluxes (up to

0.025 g m^{-2} y^{-1}). Particle diameter has been identified as one of the primary determinants, the other being density, of the settling velocity of particles, as elucidated by the principles of Stokes' Law. In our case, numerical data were produced only for one size class of BC (0.5 μm) while the mass of BC in other size classes of the atmospheric particles that are deposited at the sea surface, was not considered. It is therefore expected that our simulations should lead to both lower concentrations and fluxes.

4 Conclusions

The deposition of BC fine particles from the atmosphere to the marine area of Saronikos Gulf was investigated numerically for 2018. The contribution of the shipping industry to the overall BC 0.5 μm mass balance was estimated and found to be of low importance for the case study area, already receiving high anthropogenic pressure. The transport mechanism of the particles in the marine environment is highly influenced by the settling velocity, leading to various depositional fluxes on the seabed. Mass deposition to the seabed was higher (up to 0.025 g m^{-2} y^{-1}) when high settling velocity was selected (1 m d^{-1}). In Elefsis Bay, the concentration of PBC in the water column, as well as the mass deposited to the seabed were higher compared to open sea (station S16). The depositional fluxes and concentrations of PBC calculated within this study were lower, compared to other field studies, indicating that more sources of BC need to be included in the modelling set-up (e.g. river discharges). To further develop and validate this study, field measurements of PBC concentration in water and sediment are necessary. Deployment of sediment traps would provide a valuable source of field data information for sediment fluxes of PBC. Furthermore, biochemical interactions need to be modelled to provide a holistic approach to the fate of PBC.

Acknowledgements

This research has received funding from the NextGenerationEU under Greece's National Recovery and Resilience Plan (Greece 2.0) TAEDR-0534767 (NAVGREEN). The atmospheric datasets have been produced within EMERGE project, funded from the European Union's Horizon 2020 Research and Innovation Framework Program under Grant Agreement No 874990 (EMERGE).

References

1. Benavides, M., Chu Van, T., Mari, X. Amino acids promote black carbon aggregation and microbial colonization in coastal waters off Vietnam. Sci. Tot. Environ., 685, 527-532 (2019). https://doi.org/10.1016/j.scitotenv.2019.05.141
2. Feng, N., Yang, W.F., Zhao, X.F., Chen, M., Qiu, Y., Zheng, M. Semi-enclosed bays serve as hotspots for black carbon burial: a case study in Jiaozhou Bay, western Yellow Sea. Sci. Tot. Environ., 797(25):149100 (2021). https://doi.org/10.1016/j.scitotenv.2021.149100

3. Choomanee, P., Bualert, S., Thongyen, T., Rungratanaubon, T., Rattanapotanan, T., Szymanski W.W. Beyond common urban air quality assessment: relationship between PM2.5 and black carbon during haze and non-haze periods in Bangkok. Atmos. Pollut. Res., 15, Article 101992, (2024). https://doi.org/10.1016/j.apr.2023.101992
4. Shu, Z., Huang, C., Min, K., Long, C., Liu, L., Tan, J., Liu, Q., Jiang, G. Analysis of black carbon in environmental and biological media: Recent progresses and challenges. TrAC Trends in Analytical Chemistry. 169, 117347, (2023). https://doi.org/10.1016/j.trac.2023.117347
5. Bond, T. C., Doherty, S. J., Fahey, D. W., Forster, P. M., Berntsen, T., DeAngelo, B. J., et al. Bounding the role of black carbon in the climate system: a scientific assessment. J. Geophys. Res. 118, 5380–5552 (2013). https://doi.org/10.1002/jgrd.50171
6. Mari, X., Guinot, B., Thuoc, C.V., Brune, J., Lefebvre, J.P., Angia Sriram, P.R., Raimbault, P., Dittmar, T., Niggemann, J. Biogeochemical Impacts of a Black Carbon Wet Deposition Event in Halong Bay, Vietnam. Front. Mar. Sci. 6:185 (2019). https://doi.org/10.3389/fmars.2019.00185
7. Jurado, E., Dachs, J., Duarte, C. M., and Simóc, R. Atmospheric deposition of organic and black carbon to the global oceans. Atmos. Environ. 42, 7931–7939 (2008) https://doi.org/10.1016/j.atmosenv.2008.07.029
8. Moldanová, J., Fridell, E., Winnes, H., Holmin-Fridell, S., Boman, J., Jedynska, A., Tishkova, V., Demirdjian, B., Joulie, S., Bladt, H., Ivleva, N. P., and Niessner, R.: (2013) Physical and chemical characterisation of PM emissions from two ships operating in European Emission Control Areas, Atmos. Meas. Tech., 6, 3577–3596, (2013). https://doi.org/10.5194/amt-6-3577-2013
9. Cornelissen, G., Gustafsson, O., Bucheli, T.D., Jonker, M.T., Koelmans, A.A., van Noort, P.C. Extensive sorption of organic compounds to black carbon, coal, and kerogen in sediments and soils: mechanisms and consequences for distribution, bioaccumulation, and biodegradation. Environ Sci Technol. 39, 6881-95. (2005) https://doi.org/10.1021/es050191b
10. Long, C.M., Nascarella, M.A., Valberg, P.A. Carbon black vs. black carbon and other airborne materials containing elemental carbon: physical and chemical distinctions. Environ. Pollut, 181 (2013), 271-286. https://doi.org/10.1016/j.envpol.2013.06.009
11. Xiao, Q., Li, M., Liu, H., Fu, M., Deng, F., Lv, Z., Man, H., Jin, X., Liu, S., and He, K.: Characteristics of marine shipping emissions at berth: profiles for particulate matter and volatile organic compounds, Atmos. Chem. Phys., 18, 9527–9545, (2018). https://doi.org/10.5194/acp-18-9527-2018
12. Eger, P., Mathes, T., Zavarsky, A., and Duester, L.: Measurement report: Inland ship emissions and their contribution to NOx and ultrafine particle concentrations at the Rhine, Atmos. Chem. Phys., 23, 8769–8788, (2023). https://doi.org/10.5194/acp-23-8769-2023
13. Anderson, M., Salo, K., Hallquist, Å.M., Fridell, E. Characterization of particles from a marine engine operating at low loads. Atmos. Environ., 101, 65-71, (2015). https://doi.org/10.1016/j.atmosenv.2014.11.009
14. Rönkkö, T., Saarikoski, S., Kuittinen, N., Karjalainen, P., Keskinen, H., Järvinen, A., Mylläri, F., Aakko-Saksa, P., Timonen, H. Review of black carbon emission factors from different anthropogenic sources Environmental Research Letters, 18 (3), 033004 (2023). https://doi.org/10.1088/1748-9326/acbb1b
15. Loh, A., Kim, D., Hwang, K., An, J.G., Choi, N., Hyun, S., Yim, U.H. Emissions from ships' activities in the anchorage zone: A potential source of sub-micron aerosols in port

areas. Journal of Hazardous Materials, 457, 131775 (2023) https://doi.org/10.1016/j.jhazmat.2023.131775

16. Jalkanen, J.-P., Johansson, L., Wilewska-Bien, M., Granhag, L., Ytreberg, E., Eriksson, K. M., Yngsell, D., Hassellöv, I.-M., Magnusson, K., Raudsepp, U., Maljutenko, I., Winnes, H., and Moldanova, J.: Modelling of discharges from Baltic Sea shipping, Ocean Sci., 17, 699–728 (2021) https://doi.org/10.5194/os-17-699-2021
17. Hassellöv, I.M., Koski, M., Broeg, K., Marin-Enriquez, O., Tronczynski, J., Dulière, V., Murray, C., Bailey, S., Redfern, J., de Jong, K., Ponzevera, E., Belzunce-Segarra, M.J., Mason, C., Iacarella, J.C., Lyons, B., Fernandes, J.A. and Parmentier, K. ICES Viewpoint background document: Impact from exhaust gas cleaning systems (scrubbers) on the marine environment (Ad hoc). ICES Scientific Reports. 2:86. 40 (2020). http://doi.org/10.17895/ices.pub.7487
18. Zhang, R., Sun, B., Song, Y., Chen, X., Song, C., Wei, Z., Su, X., Zhang, C., Wu, Z. Evaluating the phytotoxicity of dissolved organic matter derived from black carbon. Sci Total Environ. 778:146231 (2021) https://doi.org/10.1016/j.scitotenv.2021.146231
19. Coppola, A.I., Ziolkowski, L.A., Masiello, C.A. & Druffel E.R.M. Aged black carbon in marine sediments and sinking particles. Geophys. Res. Lett., 41, 2427–2433 (2014). https://doi.org/10.1002/2013GL059068.
20. Yang, W., Fang, Z., Zhang, Q., Chen, M., Zheng, M. Dynamics of Particulate Black Carbon in the South China Sea: Magnitude, Resident Timescale, Sinking Speed, and Flux. Sci. Total Environ. 877, 162847 (2023). https://doi.org/10.1016/j.scitotenv.2023.162847
21. Fang, Y., Chen, Y., Huang, G., Hu, L., Tian, C., Xie, J., Lin, J., Lin, T. Particulate and Dissolved Black Carbon in Coastal China Seas: Spatiotemporal Variations, Dynamics, and Potential Implications. Environ. Sci. Technol. 55 (1), 788-796 (2021) https://doi.org/10.1021/acs.est.0c06386
22. Coppola, A.I., Druffel, E.R.M., Broek, T.A., Haghipour, N., Eglinton, T.I., McCarthy, M., Walker, B.D. Variable aging and storage of dissolved black carbon in the ocean, Proc. Natl. Acad. Sci. U.S.A. 121 (13) e2305030121 (2024) https://doi.org/10.1073/pnas.2305030121
23. Pavlidou, A., Simboura, N., Pagou, K., Assimakopoulou, G., Gerakaris, V., Hatzianestis, I., Panayotidis, P., Pantazi, M., Papadopoulou, N., Reizopoulou, S., Smith, C., Triantaphyllou, M., Uyarra, M.C., Varkitzi, I., Vassilopoulou, V., Zeri, C., Borja. A. Using a holistic ecosystem-integrated approach to assess the environmental status of Saronikos Gulf, Eastern Mediterranean. Ecol. Ind., 96, 336-350 (2019). https://doi.org/10.1016/j.ecolind.2018.09.007
24. Mazioti, A.A., Kolovoyiannis, V., Krasakopoulou, E., Tragou, E., Zervakis, V., Assimakopoulou, G., Athiniotis, A., Paraskevopoulou, V., Pavlidou, A., Zeri, C. Implementation of a Far-Field Water Quality Model for the Simulation of Trace Elements in an Eastern Mediterranean Coastal Embayment Receiving High Anthropogenic Pressure. J. Mar. Sci. Eng. 12, 797 (2024). https://doi.org/10.3390/jmse12050797
25. Tsiodra, I., Grivas, G., Bougiatioti, A., Tavernaraki, K., Parinos, C., Paraskevopoulou, D., Papoutsidaki, K., Tsagkaraki, M., Kozonaki, F.A., Oikonomou, K., Nenes, A., Mihalopoulos., N. Source apportionment of particle-bound polycyclic aromatic hydrocarbons (PAHs), oxygenated PAHs (OPAHs), and their associated long-term health risks in a major European city. Science of The Total Environment, 951, 175416 (2024). https://doi.org/10.1016/j.scitotenv.2024.175416
26. Paraskevopoulou, V., Zeri, C., Kaberi, H., Chalkiadaki, O., Krasakopoulou, E., Dassenakis, M., Scoullos, M. Trace metal variability, background levels and pollution status

assessment in line with the water framework and Marine Strategy Framework EU Directives in the waters of a heavily impacted Mediterranean Gulf. Mar. Pollut. Bull. 87, 323–337 (2014). https://doi.org/10.1016/j.marpolbul.2014.07.054

27. Jalkanen, J.-P., Fridell, E., Kukkonen, J., Moldanova, J., Ntziachristos, L., Grigoriadis, A., Moustaka, M., Fragkou, E., et al. Environmental impacts of exhaust gas cleaning systems in the Baltic Sea, North Sea, and the Mediterranean Sea area. Finnish Meteorological Institute, Helsinki, Finland. (2024) https://doi.org/10.35614/isbn.9789523361898
28. Sofiev, M., Vira, J., Kouznetsov, R., Prank, M. Soares, J., Genikhovich, E., Construction of the SILAM Eulerian atmospheric dispersion model based on the advection algorithm of Michael Galperin. Geoscientific Model Development, 8, 11, 8, 3497–3522 (2015). https://doi.org/10.5194/gmd-8-3497-2015
29. Yarwood, G., Yocke, S. R. M., and Whitten, G. (2005). Updates to the Carbon Bond Mechanism: CB05. U.S. Environmental Protection Agency, Final Report, 161 pp.
30. ECMWF (The European Centre for Medium-Range Weather Forecasts) https://www.ecmwf.int/en/forecasts/documentation-and-support/medium-range-forecasts
31. Schwarzkopf, D.A., Petrik, R., Matthias, V., Quante, M., Majamäki, E., Jalkanen, J.P. A ship emission modeling system with scenario capabilities. Atmos. Environ. X, 12, 100132, (2021). https://doi.org/10.1016/j.aeaoa.2021.100132
32. Kouznetsov, R., and M. Sofiev. A methodology for evaluation of vertical dispersion and dry deposition of atmospheric aerosols, J. Geophys. Res., 117, D01202, (2012). https://doi.org/10.1029/2011JD016366
33. Kolovoyiannis, V., Petalas, S., Mamoutos, I., Krasakopoulou, E., Zervakis, V., Tragou, E., Kontoyiannis, H. Optimizing the Parameterization of a High Resolution Numerical Simulation of the Saronikos Gulf Hydrodynamics, in: 2nd International Conference on Design and Management of Port, Coastal and Offshore Work - May 24-27 2023, Aristotle University of Thessaloniki, Greece.
34. Deltares, 2023. Delft3d-FLOW. Simulation of multi-dimensional hydrodynamic flows and transport phenomena, including sediments. User Manual, v4.05., P.O. Box 177, 2600 MH Delft, The Netherlands. Available online: https://content.oss.deltares.nl/delft3d4/Delft3D-FLOW_User_Manual.pdf (last accessed 2025/02/22)
35. Mamoutos, I.G., Potiris, E., Tragou, E., Zervakis, V., Petalas, S. A High-Resolution Numerical Model of the North Aegean Sea Aimed at Climatological Studies. J. Mar. Sci. Eng. 9, 1463 (2021). https://doi.org/10.3390/jmse9121463
36. Deltares. D-Water Quality User Manual, Water Quality and Aquatic Ecology Modelling Suite, v5.06, Deltares, P.O. Box 177, 2600 MH Delft, The Netherlands. 2020. Available online: https://content.oss.deltares.nl/delft3d4/D-Water_Quality_User_Manual.pdf (last accessed 2024/10/04)
37. Krone, R. Flume studies of transport of sediment in estuarial shoaling processes (Final report). Tech. rep., University of California, Hydraulics Engineering and Sanitary Engineering Laboratory, Berkeley, USA. (1962)
38. Ţene M., Stuparu D.E., Kurowicka D., El Serafy G.Y. A copula-based sensitivity analysis method and its application to a North Sea sediment transport model. Environ. Model. Softw., 104 (2018), pp. 1-12 https://doi.org/10.1016/J.ENVSOFT.2018.03.002
39. Jiménez, J.A., Madsen O.S. A simple formula to estimate settling velocity of natural sediments. J. Waterw. Port, Coast. Ocean Eng., 129, 70-78. (2003) https://doi.org/10.1061/(ASCE)0733-950X(2003)129:2(70)

40. Zhiyao, S., Tingting, W., Fumin, X., Ruijie, L. A simple formula for predicting settling velocity of sediment particles. Water Science and Engineering. 1, 1, 37-43. (2008) https://doi.org/10.1016/S1674-2370(15)30017-X
41. Deltares. D-Water Quality Processes Library Description, Technical Reference Manual, v5.01, Deltares, P.O. Box 177, 2600 MH Delft, The Netherlands. 2020. Available online: https://content.oss.deltares.nl/delft3d4/D-Water_Quality_Processes_Technical_Reference_Manual.pdf (last accessed 2024/10/04)
42. Fang, Z., Yang, W., Chen, M., Zheng, M., & Hu, W. Abundance and sinking of particulate black carbon in the western Arctic and Subarctic Oceans. Scientific Reports, 6(1), 1-11. (2016) https://doi.org/10.1038/srep29959